NJC

Accepted Manuscript

This is an *Accepted Manuscript*, which has been through the Royal Society of Chemistry peer review process and has been accepted for publication.

Accepted Manuscripts are published online shortly after acceptance, before technical editing, formatting and proof reading. Using this free service, authors can make their results available to the community, in citable form, before we publish the edited article. We will replace this *Accepted Manuscript* with the edited and formatted *Advance Article* as soon as it is available.

You can find more information about *Accepted Manuscripts* in the Information for Authors.

Please note that technical editing may introduce minor changes to the text and/or graphics, which may alter content. The journal's standard Terms & Conditions and the Ethical guidelines still apply. In no event shall the Royal Society of Chemistry be held responsible for any errors or omissions in this *Accepted Manuscript* or any consequences arising from the use of any information it contains.

ROYAL SOCIETY OF CHEMISTRY

www.rsc.org/njc

Journal Name

RSCPublishing

ARTICLE

One-step Synthesis of SnO_2 Nanoparticles-Loaded Graphitic Carbon Nitride and their Application in Thermal Decomposition of Ammonium Perchlorate

Qi Li,[a] Yi He*[b] and Rufang Peng*[a]

Cite this: DOI: 10.1039/xoxxoooooox

Received ooth January 2012,
Accepted ooth January 2012

DOI: 10.1039/xoxxoooooox

www.rsc.org/

SnO_2 nanoparticles-loaded graphitic carbon nitride (SnO_2NPs/g-C_3N_4) hybrids were successfully synthesized by one-pot calcining. Various characterization means and detection techniques were used to analyse their structure and properties. It was found that SnO_2 NPs possess the synergistic effect on g-C_3N_4. The addition of SnO_2 NPs not only increases the surface of g-C_3N_4 but provide extra electron. Having added 10 wt% SnO_2NPs/g-C_3N_4 hybrids, the onset decomposition temperature of ammonium perchlorate (AP) was decreased to 352.2 °C. Furthermore, considering the band gap of g-C_3N_4 (Eg = 2.7 eV) and SnO_2 (Eg = 3.6 eV), the conduction band electrons (e_{cb}^-) and valence band holes (h^+) were generated on their surface under heat excitation. In addition, on the basis of the synergistic effect (the e_{cb}^- would transfer from g-C_3N_4 to SnO_2) of SnO_2, a possible synergistic mechanism was proposed to understand the thermal decomposition of AP.

Introduction

Composite solid propellants (CSPs) have a significant effect on the properties of rockets and missiles, such as onset decomposition temperature and burning rates. Now, the CSP are generally composed of prepolymer (binder), high energy fuel, and oxidizer salts.[1,2] Ammonium perchlorate (AP) is a kind of common oxidants, which has been widely used in various propellants. The burning behaviours of CSPs are strongly dependent on the properties of AP decomposition. The lower high-temperature decomposition (HTD) temperature and decomposition heat of AP can lead to a shorter ignition delay time and a higher burning rate.[3,4] In this regard, to improve the oxidation effects of AP, various catalysts were explored to catalyse AP so as to decrease its onset decomposition temperature. The most commonly used catalysts are metal oxidation until now, such as CuO,[5] CoO,[6] $CuFe_2O_4$,[7] Co_3O_4,[8] ZnO,[9] LDH/C,[10] MnO_2,[11] Mn_3O_4,[12] $MgAl_2O_4$,[13] and NiO,[14] which could decrease the onset decomposition temperature of AP decomposition to a certain extent. Nevertheless, these existing catalysts possess many disadvantages, for example, low production, complicated preparation process, and high cost, giving rise to environmental pollution as well as extremely limit their large-scale applications in propellants and missiles. Therefore, one way to overcome the disadvantages is to develop novel catalysts with high efficiency, low cost and easy preparation.

Lately, graphitic carbon nitride (g-C_3N_4) has been significantly concerned because of its characteristics and special properties, such as earth-abundant, metal-free, low band gap, etc.[15-18] In addition, taking into account the band gap of g-C_3N_4 (Eg = 2.7 eV), it can absorb blue-violet light when wavelength lower than 475 nm of solar spectrum.[19,20] On this basis, g-C_3N_4 has been widely applied in solar water splitting and thermal decomposition of AP.[21-25] Meanwhile, the research of surface modification of g-C_3N_4 has attracted much attention due to its excellent performances. For example, Shloam et al. reported that SiO_2NPs/g-C_3N_4 composite was successfully prepared and it was applied to the degradation of organic pollutions (rhodamine B).[26] Obviously, g-C_3N_4-based materials possess wide application foreground in photo-catalysis, sensing and bio-imaging.[27,28] However, g-C_3N_4-based materials as a heat catalyst for AP decomposition have not been reported.

Herein, for the first time, we reported that SnO_2NPs/g-C_3N_4 hybrids were successfully prepared as well as discovered that the hybrids could be used as a novel catalyst in AP decomposition. In particular, SnO_2NPs/g-C_3N_4 hybrids could effectively decrease the HTD temperature by 102.2 °C. Furthermore, SnO_2, as a good semiconductor (Eg = 3.6 eV),[29] possess synergistic effect on the g-C_3N_4. As a consequence, we proposed a possible synergistic mechanism for the decomposition of AP. Namely, the generated conduction band electron (e_{cb}^-) on the g-C_3N_4 would transfer to the surface of SnO_2. Besides, the generated e_{cb}^- and h^+ can react with $HClO_4$ and NH_4 which is originated from the lattice of AP, pushing the reaction to proceed toward the right hand of reversible reaction of AP decomposition. On the other hand, SnO_2NPs/g-C_3N_4 hybrids provide the possibility of large-scale applications in the industry field.

Experimental section

Chemicals and apparatus

Dicyandiamide (DCDA, 99%), SnO_2 (99.9%, 30-50 nm) and ammonium perchlorate (AR, d_{50}:135 μm) were purchased from Aladdin (Shanghai, China). Tubular furnace atmosphere was obtained from Zhonghuan experiment electric furnace (Tianjin, China). All reagents are of analytic grade and used without further purification.

Preparation of SnO_2NPs/g-C_3N_4 hybrids

The SnO_2NPs/g-C_3N_4 hybrids were prepared via a modified general method according to earlier study.[30] Typically, the powder of SnO_2NPs and DCDA (molar ratio equal 1:1) was fully mixed to grind for 30 minutes ("fully mixed" was key to the decrease of agglomeration degree). Finally, the mixture was placed in the tubular furnace atmosphere and calcined at 550 °C under argon flow with a heating rate of 2.5 K•min^{-1}.

Characterization

The samples were characterized by X-ray powder diffraction (XRD) with Philips X'Pert Pro X-ray diffractometer equipped with Cu Kα radiation (λ = 0.15418 nm). Field-emission scanning electron microscopy (FESEM) image was performed on Ultra (Carl Zeiss, German) with an acceleration voltage of 15.0 kV. Field-emission transmission electron microscopy (FETEM) images were carried out on Libra 200FE (Carl Zeiss, German). Fourier transform infrared (FT-IR) spectra were recorded on a Nicolet-5700 FTIR spectrometer using pressed KBr pellets to test the chemical bonding of the samples from 4000 to 400 cm^{-1}. X-ray photoelectron spectra (XPS) were acquired on an ESCALAB MKII with Mg Kα (hν = 1253.6 eV) as the excitation source.

Catalytic measurements

To test the catalytic activities of SnO_2NPs/g-C_3N_4 hybrids in the thermal decomposition of AP, AP mixed with the SnO_2, g-C_3N_4 and SnO_2NPs/g-C_3N_4 hybrids were ground for 30 min, respectively. The resulting mixture was detected by thermo-gravimetric/differential thermal analysis/differential scanning calorimetry (TG/DTA/DSC) using SDT Q600 (TA, America) at a heating rate of 10 °C•min^{-1} in a static N_2 atmosphere over the temperature range of 25-500 °C. Thermal gravity analysis-Fourier transform infrared (TGA-FTIR), as a special detection means, was used to analyse catalytic mechanism of the thermal decomposition of AP by real-time detecting the products.

Results and discussion

Characterization of SnO_2NPs/g-C_3N_4 hybrids

The schematic of preparation of SnO_2NPs/g-C_3N_4 hybrids was indicated in Fig. S1. The structure of as-prepared SnO_2NPs/g-C_3N_4 hybrid was characterized by XRD. As shown in Fig. 1a, the respective XRD peaks of g-C_3N_4 and SnO_2 can be observed, respectively. The parameters of g-C_3N_4 and SnO_2 are consistent with the literature values of JCPDS No. 87-1526 and No. 70-4175, respectively. For the XRD pattern of SnO_2, the peaks located at 26.5°, 33.8°, 37.9° and 51.7° are correspond to (110), (101), (200) and (211), respectively. Toward the g-C_3N_4, the peak located at 27.3° is corresponded to the interlayer diffraction of graphitic-like structures and the peak at 13.3° is ascribed to in-planar repeated triazine units, respectively. It should be noted that SnO_2NPs/g-C_3N_4 hybrids show the diffraction peaks located at 13.3°, 26.5°, 27.3°, 33.8°, 37.9° and 51.7°, which are consistent with the characteristic peaks of SnO_2 and g-C_3N_4, indicating the existence of SnO_2 in the as-prepared SnO_2NPs/g-C_3N_4 hybrids.

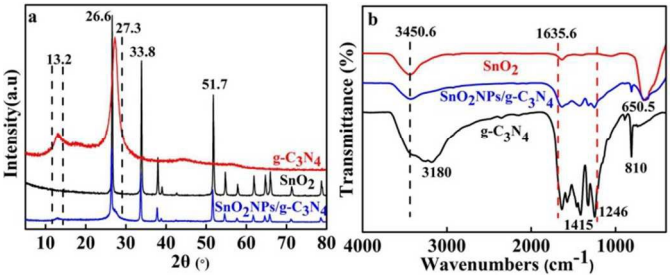

Fig. 1 (a) XRD patterns of g-C_3N_4, SnO_2 NPs and SnO_2NPs/g-C_3N_4 hybrids. (b) FT-IR spectra of g-C_3N_4, SnO_2 NPs and SnO_2NPs/g-C_3N_4 hybrids.

XRD results were further confirmed by FT-IR investigation. Fig. 1b shows the FT-IR spectra of three samples. As to pure SnO_2 NPs, the relatively broad peak centred at 3450.6 cm^{-1} is ascribed to water molecules of crystallization. The sharp peak at 650.5 cm^{-1} is characteristic peak of the SnO_2 crystallization.[31, 32] Moreover, for the g-C_3N_4, the peaks at 1246, 1415, and 1636 cm^{-1} are attributed to the typical stretching modes of CN heterocycles.[17,24] The peaks between 3000 and 3400 cm^{-1} are ascribed to the secondary and primary amines.[25] Notably, for SnO_2NPs/g-C_3N_4 hybrids, all of peaks of SnO_2 NPs and g-C_3N_4 can be observed, suggesting the formation of SnO_2NPs/g-C_3N_4 hybrids.

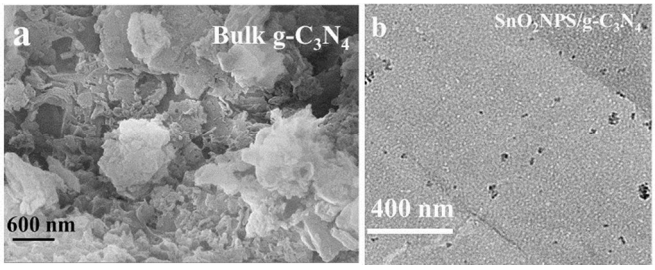

Fig. 2 (a) FESEM image of bulk g-C_3N_4, (b) TEM image of SnO_2NPs/g-C_3N_4 hybrids.

The morphology of as-prepared bulk g-C_3N_4 and SnO_2NPs/g-C_3N_4 hybrids were confirmed by FESEM and TEM images. In contrast to the bulk g-C_3N_4 (Fig. 2a), it can be clearly seen that SnO_2 NPs were dispersed on the surface of g-C_3N_4 sheets (Fig. 2b). What's more, the degree of agglomeration is relatively less. As shown in Fig. S2, it should be noted that the addition of SnO_2 NPs increase the g-C_3N_4 surface up to 11.8 m^2•g^{-1}, which was 4 times larger than that of bulk g-C_3N_4 (2.9 m^2•g^{-1}).[30] Compared with SnO_2NPs/g-C_3N_4 hybrids (prepared by different ratios of SnO_2NPs and DCDA), the BET of SnO_2NPs/g-C_3N_4 hybrids is larger than hybrids 2 (Fig. S2c) and 3 (Fig. S2d), confirming that the molar ratios of 1:1 between SnO_2NPs and DCDA is the best. Above discussions demonstrated the formation of SnO_2NPs/g-C_3N_4 hybrids. To further probe the chemical environment and chemical composition of the as-

prepared hybrids, XPS measurements were performed. As indicated in Fig. 3a, SnO_2, the typical Sn $3d_{5/2}$ (486.5 eV), Sn $3p_{3/2}$ (716 eV), Sn Auger (1049.6 eV) and O 1s (530.7 eV) peaks were observed, which were accord in the result of previously reported literature.[33] As to g-C_3N_4, two strong peaks of C 1s (285.9 eV) and N 1s (399.6 eV) were in previous studies.[19] Particularly, for the as-prepared SnO_2NPs/g-C_3N_4 hybrids, C, N, O, and Sn were distinctly seen in the spectroscopy. In the high-resolution N 1s XPS spectroscopy of g-C_3N_4 (Fig. 3c), the peaks located at 396.2 and 397.3 eV are corresponded to sp2 C-N=C and sp3 N-[C],[3] respectively. However, in contrast to N 1s of g-C_3N_4, the high-resolution N 1s spectroscopy of SnO_2NPs/g-C_3N_4 hybrids shows the obvious differences. The appearance of peak at 398.8 eV and a positive shift (0.5 eV) of the peak of nitrogen atoms in the C-N=C group (396.7 eV) confirmed that the existence of reaction between SnO_2 and g-C_3N_4.

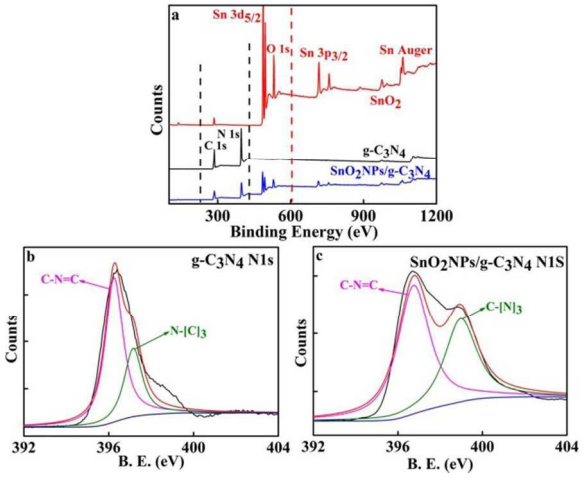

Fig. 3 (a) XPS survey spectra of SnO_2, g-C_3N_4 and SnO_2NPs/g-C_3N_4 hybrids. (b) High-resolution N 1s spectroscopy of g-C_3N_4 and (c) SnO_2NPs/g-C_3N_4 hybrids.

Catalytic activities of SnO_2NPs/g-C_3N_4 hybrids in thermal decomposition of AP

In order to detect the catalytic activities of the as-prepared SnO_2NPs/g-C_3N_4 hybrids in thermal decomposition of AP, AP mixed with g-C_3N_4, SnO_2 NPs and SnO_2NPs/g-C_3N_4 hybrids were tested by DSC and DTA measurements, respectively. As indicated in Fig. S3, to the DSC curve of pure AP decomposition, the single endothermic peak at 245.5 °C is corresponded to the crystallographic transition of AP.[3] The first exothermic peak at 338.9 °C and 454.4 °C are attributed to the low-temperature decomposition (LTD), and HTD, respectively.[4,34] Compared with the pure AP, DSC curve of AP mixed with g-C_3N_4 exhibits the HTD temperature located at 384.4 °C, confirming that g-C_3N_4 possess the intrinsic catalytic effect on AP (Fig. S3).[24] SnO_2, as a semiconductor, displays the catalytic effect on the AP (Fig. 4a). However, DSC curve of AP mixed with 10 wt% SnO_2NPs/g-C_3N_4 hybrids displays a single exothermic peak and the HTD temperature was decreased to 352.2 °C (Fig. 4b). The obvious change highlights the promoting effect of SnO_2, which improved the catalytic performance of g-C_3N_4 for the thermal decomposition of AP. Fig. 4c and Fig. 4d show the TG-DTG curve of AP mixed with SnO_2 NPs, SnO_2NPs/g-C_3N_4 hybrids, respectively. It can be seen from Fig. 4c that two-step loss weight can be observed from the DTG curve of AP mixed with SnO_2 and the exothermic peak cantered at 408.1 °C is consistent with the DTA curve. However, compared with the two-step loss weight of DTG curve (Fig. 4c), Fig. 4d shows a one-step loss weight and further suggested that SnO_2NPs/g-C_3N_4 hybrids possess excellent catalytic effect. In addition, the temperature differences and decomposition heat of HTD of AP and AP mixed with three additives of g-C_3N_4, SnO_2 and SnO_2NPs/g-C_3N_4 are shown in Fig. 4e and Fig. 4f, respectively. Moreover, as shown in Fig. S4, the TGA-DTG curves confirmed that the temperature of high temperature decomposition decreased with the increase of the molar ratio SnO_2 and dicyandiamide. All the results manifested that SnO_2NPs/g-C_3N_4 hybrid is a good catalyst in the thermal decomposition of AP.

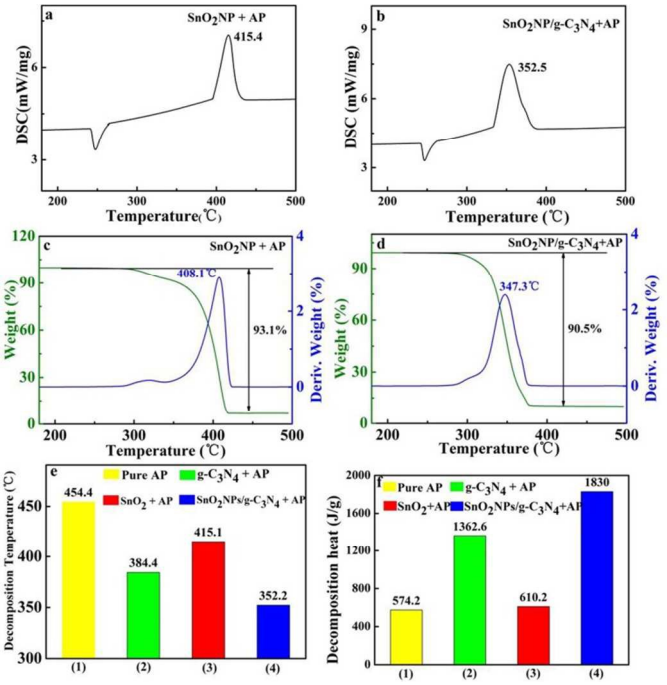

Fig. 4 (a) DSC curves of AP mixed with SnO_2 NPs. (b) DSC curves of AP mixed with SnO_2NPs/g-C_3N_4 hybrids. (c) TG-DTG curve of AP mixed with SnO_2 NPs and (d) SnO_2NPs/g-C_3N_4 hybrids. (e) Decomposition temperature of AP and (f) decomposition heat of AP with the three additives of g-C_3N_4, SnO_2 NPs and SnO_2NPs/g-C_3N_4 hybrids.

Catalytic mechanisms

Jacobs[35] proposed the mechanism of AP thermal decomposition for the first time. The details as follows:

$$NH_4^+ClO_4^- \rightleftharpoons NH_3 - H - ClO_4 \rightleftharpoons NH_3 - HClO_4 \rightleftharpoons NH_{3(a)} + HClO_{4(a)} \quad (LTD) \quad (1)$$

$$NH_{3(a)} + HClO_{4(a)} \rightleftharpoons NH_{3(g)} + HClO_{4(g)} \quad (HTD) \quad (2)$$

As is well-known, the pair of ions (NH_4^+ and ClO_4^-) in the $NH_4^+ClO_4^-$ lattice. The LTD was confirmed to be a heterogeneous process which the proton was transferred from NH_4^+ to ClO_4^-, leading to the formation of NH_3(a) and $HClO_4$(a). Subsequently, in the HTD process, the gas-phase molecule of NH_3 and $HClO_4$ would separate from the AP lattice and resulting in decomposition of $HClO_4$ and NH_3.[6,35] Obviously, the exothermic process of HTD is owing to the oxidation of NH_3 and reduction of $HClO_4$.[3,36]

So, how could SnO_2NPs/g-C_3N_4 hybrids catalyse the AP decomposition? As can be seen from the eq. (1) and eq. (2), the adsorption of $HClO_4$ and NH_3 on the AP surface during LTD process as well as the reduction of $HClO_4$ plays a key role in thermal decomposition of AP. In primary decomposition stage of AP, the adsorption of $HClO_4$ in the pores of AP prevented the decomposition of AP because the eq. (2) is reversible.[37] On the other hand, g-C_3N_4, as a Lewis base, can react with $HClO_4$ by Lewis acid-base interaction, leading to the separation of $HClO_4$ from the pores of AP as well as pushing the decomposition reaction to proceed toward the right-hand side of the eq. (2). The evidence of reaction between g-C_3N_4 and $HClO_4$ was shown in Fig. S5. For the FT-IR spectrum of g-C_3N_4 and the treated g-C_3N_4 with $HClO_4$, there was an obvious change occurred. The peaks at 1146, 1120 and 1096 cm^{-1} are the characteristic peaks of ClO_4^-.[24] Therefore, it was found that Lewis acid-base reaction is involved in the thermal decomposition of AP.

On the other hand, g-C_3N_4, as a polymer semiconductor (Eg =2.7 eV), is easy to meet the requirements of heat excitation.[38] Thus, the e_{cb}^- and h^+ could be generated on the surface of g-C_3N_4 under heat excitation.[17,27] In addition, in view of the synergistic effect of SnO_2, the generated electron on g-C_3N_4 would transfer to the SnO_2. Therefore, the electrons and holes were separated; the probability of composite between electrons and holes would decrease to some extent. Clearly, the remaining electrons and holes would participate in the reduction of perchlorate acid and oxidation of ammonium. The conclusion was similar to the previous literature.[39] During the decomposition process, e_{cb}^- could react with $HClO_4$, causing the reduction of $HClO_4$ and production of $\bullet O_2^-$. The generation of $\bullet O_2^-$ was demonstrated by electron paramagnetic resonance spectroscopy (EPR) and thermal analysis experiments (Fig. S6 and Fig. S7). Finally, $\bullet O_2^-$ and h^+ with powerful oxidation ability could further react with NH_3 to form N_2O, NO_2 and H_2O,[16] leading to the continue decomposition of AP because the decomposition process is reversible.

The gas products during AP decomposition were further confirmed by TGA-FTIR instrument with real-time monitoring. Fig. 5 shows the three-dimensional TGA-FTIR spectra of thermal decomposition of AP mixed with SnO_2NPs/g-C_3N_4 hybrids.

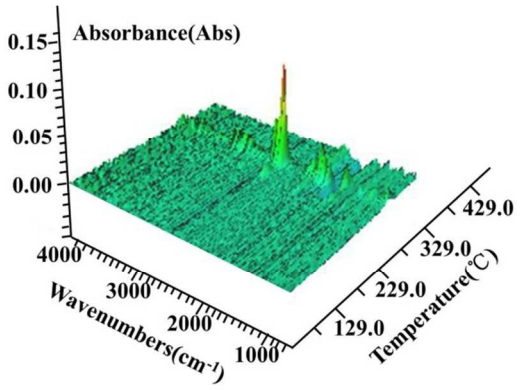

Fig. 5 Three-dimensional TGA-FTIR spectra of the thermal decomposition of AP mixed with SnO_2NPs/g-C_3N_4 hybrids.

As shown in Fig. 6, FT-IR spectra of the gas products in AP thermal decomposition was used to analyse gas composition. All of the gas products are origin from the LTD and HTD process (290-320 °C and 330-380 °C). The gas products at 368 °C were identified as H_2O, NH_3 (1650-1620 cm^{-1} and 3400-3650 cm^{-1}), HCl (1750-3000 cm^{-1}), N_2O, NO_2 (2202-2238 cm^{-1}, 1380-1320 cm^{-1} and 840-800 cm^{-1}) and ClO_3 (1000-900 cm^{-1}).[24] In addition, the gas products of decomposition temperature at 398, 348 and 288 °C were also demonstrated the production of the above gas.

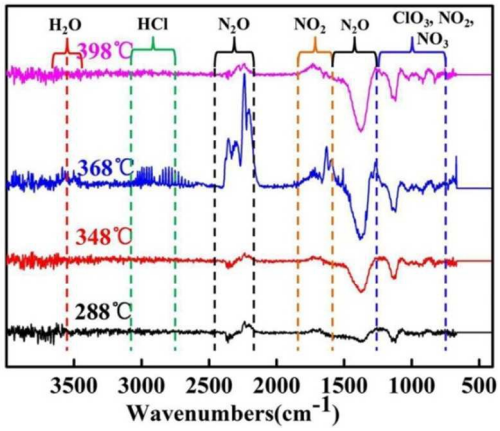

Fig. 6 FTIR spectra of gas products during the thermal decomposition of AP mixed with SnO_2NPs/g-C_3N_4 hybrids.

In short, SnO_2NPs/g-C_3N_4 hybrid as the catalyst for the thermal decomposition of AP is shown in Fig. 7.

In short, the schematic of thermal decomposition of AP is shown in Fig. 7 (SnO_2NPs/g-C_3N_4 hybrid as the heat catalyst).

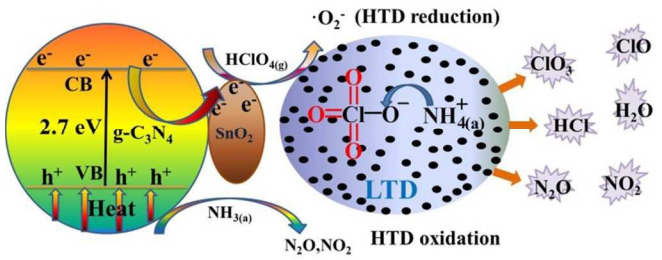

Fig. 7 Schematic of the thermal decomposition process of AP with the additive of SnO_2NPs/g-C_3N_4 hybrids.

Conclusions

In summary, SnO_2NPs/g-C_3N_4 hybrids were successfully prepared. It was proved that the as-prepared hybrids could be used as an excellent catalyst for AP thermal decomposition. When SnO_2NPs/g-C_3N_4 hybrid was added to AP, the HTD temperature of AP was decreased by 102.2 °C. Furthermore, a possible synergistic mechanism was proposed to illustrate the thermal decomposition of AP. Moreover, SnO_2NPs/g-C_3N_4 hybrid as a novel catalyst provided a new insight for the preparation of other g-C_3N_4-based functional materials and the thermal decomposition of AP.

Acknowledgements

This work was supported by the Natural Science Foundation of China (51372211, 10576026 and 21301142), Defence Science and Technology Project (A3120133002), Youth Innovation Research Team of Sichuan for Carbon Nanomaterial (2011JTD0017), and Postgraduate Innovation Fund Project by Southwest University of Science and Technology (15ycx007).

Notes and references

[a] *State Key Laboratory Cultivation Base for Non-metal Composites and Functional Materials, Southwest University of Science and Technology, Mianyang 621010, P, R, China*
Fax: +86-816-2419011; Tel: +8613547133920;
Email: pengrufang@swust.edu.cn
[b] *School of National Defence Science and Technology, Southwest University of Science and Technology, Mianyang, 621010, P, R, China*
Email: yhe2014@126.com

(1) Jacobs, P. W. M.; Whitehead, H. M.; *Chem. Rev*. **1969**, 69, 551-590.
(2) Kapoor, I. P. S.; Srivastava, P.; Singh, G. *Propellants Explos. Pyrotech*. **2009**, 34, 351-356.
(3) Boldyrev, V.; *Thermochim. Acta*. **2006**, 443, 1-36.
(4) Vyazovkin, S.; Wight, C. A.; *Chem. Mater*. **1999**, 11, 3386-3393.
(5) Chen, L.; Li, G.; Li, L. *J. Therm. Anal. Cal*. **2008**, 91, 581-587.
(6) Li, L.; Sun, X.; Qiu, X.; Xu, J.; Li, G. *Inorg. Chem*. **2008**, 47, 8839-8846.
(7) Liu, T.; Wang, L.; Yang, P.; Hu, B. *Mater. Lett*. **2008**, 62, 4056-4058.
(8) Lu, S.; Jing, X.; Liu, J.; Wang, J.; Liu, Q.; Zhao, Y.; Jamil, S.; Zhang, M.; Liu, L. *J. Solid State. Chem*. **2013**, 197, 345-351.
(9) Tang, G.; Tian, S.; Zhou, Z.; Wen, Y.; Pang, A.; Zhang, Y.; Zeng, D.; Li, H.; Shan, B.; Xie, C. *J. Phys. Chem. C*. **2014**, 118, 11833-11841.
(10) Li, Z.; Xiang, X.; Bai, L.; Li, F. *Appl. Clay Sci*. **2012**, 65-66, 14-20.
(11) Chandru, R. A.; Patra, S.; Oommen, C.; Munichandraiah, N. Raghunandan, B. N. *J. Mater. Chem*. **2012**, 22, 6536-6538.
(12) Li, N.; Geng, Z.; Cao, M.; Ren, L.; Zhao, X.; Liu, B.; Tian, Y.; Hu, C. *Carbon*. **2013**, 54, 124-132.
(13) Guan, X.; Li, L.; Zheng, J.; Li, G. *RSC Adv*. **2011**, 1, 1808-1814.
(14) Wang, Y.; Zhu, J.; Yang, X.; Lu, L.; Wang, X. *Thermochim. Acta*. **2005**, 437, 106-109.
(15) Sekine, T.; Kanda, H.; Bando, Y.; Yokoyama, M. *J. Mater. Sci. Lett*. **1990**, 9, 1376-1378.
(16) Wang, X.; Blechert, S.; Antonietti, M. *ACS Catal*. **2012**, 2, 1596-1606.
(17) Wang, X.; Chen, X.; Thomas, A.; Fu, X.; Antonietti, M, *Adv. Mater*. **2009**, 21, 1609-1612.
(18) Wang, Y.; Zhang, J.; Wang, X.; Antonietti, M.; Li, H. *Angew. Chem. Int. Ed*. **2010**, 49, 3356-3359.
(19) Wang, X.; Maeda, K.; Thomas, A.; Takanabe, K.; Xin, G.; Carlsson, J. M.; Domen, K.; Antonietti, M. *Nat. Mater*. **2009**, 8, 76-80.
(20) Thomas, A.; Fischer, A.; Goettmann, F.; Antonietti, M.; Müller, J. O.; Schlögl, R.; Carlsson, J. M. *J. Mater. Chem*. **2008**, 18, 4893-4908.
(21) Jrgens, B.; Irran, E.; Senker, J.; Kroll, P.; Mller, H.; Schnick, W. *J. Am. Chem. Soc*. **2003**, 125, 10288-10300.
(22) Grey, C. P.; Dupré, N. *Chem. Rev*, **2004**, 104, 4493-4512.
(23) Algara-Siller, G.; Severin, N.; Chong, S. Y.; Björkman, T.; Palgrave, R. G. Laybourn, A.; Antonietti, M.; Khimyak, Y. Z.; Krasheninnikov, A. V.; Rabe, J. P.; Kaiser, U.; Cooper, A. I.; Thomas, A.; Bojdys, M. J. *Angew. Chem. Int. Ed*. **2014**, 53, 7450-7455.
(24) Li, Q.; He, Y.; Peng, R. *RSC Advances*. **2015**, 5, 24507-24512.
(25) Ma, T.; Tang, Y.; Dai, S.; Qiao, S. *Small*. **2014**, 10, 2382-2389.
(26) Shalom, M.; Inal, S.; Neher, D.; Antonietti, M. *Catal. Today*. **2014**, 225, 185-190.
(27) Zhang, L.; Jing, D.; She, X.; Liu, H.; Yang, D.; Lu, Y.; Li, L.; Zheng, Z.; Guo, L. *J. Mater. Chem. A*. **2013**, 2, 2071-2078.
(28) Martin, D. J.; Qiu, K.; Shevlin, S. A.; Handoko, A. D.; Chen, X.; Guo, Z.; Tang, J. *Angew. Chem. Int. Ed*. **2014**, 53, 9240-9245.
(29) Zhu, H.; Yang, D.; Yu, G.; Zhang, H.; Yao, K. *Nanotechnology*. **2006**, 17, 2386-2389.
(30) Lu, X.; Xu, K.; Chen, P.; Jia, K.; Liu, S.; Wu, C. *J. Mater. Chem. A*. **2014**, 44, 18924-18928.
(31) Zhou, J.; Zhang, M.; Hong, J.; Fang, J.; Yin, Z. *Appl. Phys. A*. **2004**, 81, 177-182.
(32) Katiyar, R. S.; Dawson, P.; Hargreave, M.; Wilkinson, G. R. *J. Phys. C: Solid State Phys*. **1971**, 4, 2421-2432.
(33) Ansell, R. O.; Dickson, T.; Povey, M. F.; Sherwood, P. M. A. *J. Electronchem. Soc*. **1977**, 124, 1360-1364.
(34) Reid, D. L.; Russo, A. E.; Carro, R. V.; Stephens, M. A.; LePage, A. R.; Spalding, T. C. *Nano Lett*. **2007**, 7, 2157-2161.
(35) Jacobs, P. W. M.; Russell-Jones, A. J. Phys. Chem. **1968**, 72, 202-207.
(36) Khairetdinov, E. F.; Boldyrev, V. V. *Thermochim. Acta*. **1980**, 41, 63-86.

(37) Shen, G. Z.; Chen, D.; Lee, C. J. *J. Phys. Chem. B*. **2006**, 110, 15689-15693.
(38) Stoneham, A. M. *Rep. Prog. Phys*. **1981**, 44, 1251-1295.
(39) Cheng, N. Y.; Tian, J. Q.; Liu, Q.; Ge, C. J.; Qusti, A. H.; Asiri, A. M. *ACS Appl. Mater. Interfaces*. **2013**, 5, 6815-6819.